Large Cross-Section Enhancement and Intramolecular Energy Transfer upon Multiphoton Absorption of Hindered Diphenylaminofluorene-C_{60} Dyads and Triads

Prashant A. Padmawar,[†] Joy E. Rogers,[‡] Guang S. He,[§] Long Y. Chiang,*[,†] Loon-Seng Tan,*[,‡] Taizoon Canteenwala,[†] Qingdong Zheng,[§] Jonathan E. Slagle,[‡] Daniel G. McLean,[‡] Paul A. Fleitz,[‡] and Paras N. Prasad[§]

Department of Chemistry, University of Massachusetts Lowell, Lowell, Massachusetts 01854, AFRL/ML, Air Force Research Laboratory, Wright-Patterson Air Force Base, Dayton, Ohio 45433, and Institute for Lasers, Photonics and Biophotonics, and Department of Chemistry, State University of New York, Buffalo, New York 14260

Received March 26, 2006. Revised Manuscript Received June 17, 2006

Sterically hindered fullerenyl chromophore dyad and triads, $C_{60}(>\text{DPAF-C}_9)_x$ ($x = 1$ and 2, respectively), in an acceptor−donor (A−D) molecular linkage of C_{60}-(*keto*-fluorene)$_x$ were synthesized and fully characterized. Attachment of two 3,5,5-trimethylhexyl groups on C_9 of the fluorene ring moiety greatly improves their solubility and makes direct intermolecular aromatic stacking contacts more difficult. They are the *first* series of fullerene derivatives showing high three-photon absorptivity (3PA). Accordingly, $C_{60}(>\text{DPAF-C}_9)_2$ exhibits 2PA and 3PA cross sections in the values of 0.824×10^{-48} cm^4 s (or 82.4 GM) and 6.30×10^{-25} cm^6/GW^2, respectively, in femtosecond region among the highest ones reported for many diphenylaminofluorene-derived AFX chromophores. Utilization of a keto linker located immediately between C_{60} cage and fluorene chromophore moieties facilitates molecular polarization of the DPAF ring toward the C_{60} cage. That may serve as the fundamental cause for correlation of enhanced A−D electron interactions to, ultimately, observed multiphoton absorption cross sections. By using nanosecond laser flash photolysis results taken at 355 nm as the reference, transient absorption data obtained from femtosecond pump−probe experiments at 800 nm unambiguously verified the occurrence of two-photon excitation processes of $C_{60}(>\text{DPAF-C}_9)$ in air-saturated benzene and subsequent efficient energy transfer from the two-photon pumped DPAF-C_9 moiety to the C_{60} cage moiety.

Introduction

Fullerene derivatives are electron acceptor compounds. In addition to extensive interest in these materials for the fabrication of organic photovoltaic devices,[1] there were numerous reported studies focused on nonlinear optical responses of C_{60} and its monoadducts that made them good component candidates in the materials design for laser and sensor protection coatings[2] and all-optical switching devices.[3] An example of the latter case, demonstrated by cross-linked polyurethane films containing a high content of covalently bonded C_{60} monoadduct, was found to exhibit a large third-order optical nonlinearity within the telecommunication range of 1150−1600 nm.[4] The origin of its optical nonlinearity arises from unique fullerenyl excited states upon photoactivation. Nearly quantitative efficiency of intersystem crossing from the singlet excited state of C_{60} to its triplet excited state makes the latter highly populated immediately after photoexcitation. That significantly increases triplet−triplet (T_1-T_n) transient absorption cross sections and, thus, its ability to absorb more light at this excited state than the ground state. The phenomena become the foundation and source of reverse saturable absorption (RSA) properties detected for many fullerene derivatives and C_{60}-containing polymers.[5] While a number of C_{60} monoadducts have been proven to possess promising second-order nonlinear optical

* Corresponding author e-mail: Long_chiang@uml.edu.
[†] University of Massachusetts Lowell.
[‡] Wright-Patterson Air Force Base.
[§] Institute for Lasers, Photonics and Biophotonics.

(1) Segura, J. L.; Martin, N.; Guldi, D. M. *Chem. Soc. Rev.* **2005**, *34* (1), 31−47.
(2) (a) Tutt, L. W.; Kost, A. *Nature* **1992**, *356*, 225. (b) Justus, B. L.; Kafafi, Z. H.; Huston, L. *Opt. Lett.* **1993**, *18*, 1603. (c) Joshi, M. P.; Mishra, S. R.; Rawat, H. S.; Mehendale, S. C.; Rustagi, K. C. *Appl. Phys. Lett.* **1993**, *62*, 1763. (d) Li, C.; Si, J.; Yang, M.; Wang, R.; Zhang, L. *Phys. Rev. A* **1995**, *51*, 569. (e) Gvishi, R.; Bhawalker, J. D.; Kumar, N. D.; Ruland, G.; Narang, U.; Prasad, P. N. *Chem. Mater.* **1995**, *7*, 2199. (f) Maggini, M.; Scorrano, G.; Prato, M.; Brusatin, G.; Innocenzi, P.; Guglielmi, M.; Renier, A.; Signorini, R.; Meneghetti, M.; Bozio, R. *Adv. Mater.* **1995**, *7*, 404. (g) Smilowitz, L.; McBranch, D.; Klimov, V.; Robinson, J. M.; Koskelo, A.; Grigorova, M.; Mattes, B. R.; Wang, H.; Wudl, F. *Opt. Lett.* **1996**, *21*, 922. (h) Sun, Y.-P.; Riggs, J. E. *J. Chem. Soc., Faraday Trans.* **1997**, *93*, 1965. (i) Sun, Y.-P.; Riggs, J. E. *Chem. Mater.* **1997**, *9*, 1268.
(3) Stegeman, G. I.; Miller, A. In *Photonics in Switching, Vol. 1*; Midwinter, J. E., Ed.; Academic Press: San Diego, CA, 1993.
(4) (a) Kuang, L.; Chen, Q.; Sargent, E. H.; Wang, Z. Y. *J. Am. Chem. Soc.* **2003**, *125*, 13648−13649. (b) Chen, Q.; Kuang, L.; Sargent, E. H.; Wang, Z. Y. *Appl. Phys. Lett.* **2003**, *83*, 2115−2117. (c) Chen, Q.; Kuang, L.; Wang, Z. Y.; Sargent, E. H. *Nano Lett.* **2004**, *4*, 1673−1675.
(5) For a general discussion of reverse saturable properties and materials, see (a) Perry, J. W. In *Nonlinear Optics of Organic Molecules and Polymers*; Nalwa, H. S., Miyata, S., Eds.; CRC: Boca Raton, FL, 1997; pp. 813−840. (b) Said, A. A.; Wamsley, C.; Hagan, D. J.; van Stryland, E. W.; Reinhardt, B. A.; Roderer, P.; Dillard, A. G. *Chem. Phys. Lett.* **1994**, *228*, 646−650. (c) Sun, Y.-P.; Lawson, G. E.; Riggs, J. E.; Ma, B.; Wang, N.; Moton, D. K. *J. Phys. Chem. A* **1998**, *102*, 5520−5528. (d) Maggini, M.; Faveri, C. D.; Scorrano, G.; Prato, M.; Brusatin, G.; Guglielmi, M.; Meneghetti, M.; Signorini, R.; Bozio, R. *Chem.−Eur. J.* **1999**, *5*, 2501−2510. (e) Spangler, C. W. *J. Mater. Chem.* **1999**, *9*, 2013−2020.

10.1021/cm060718z CCC: $33.50
Published on Web 07/28/2006

properties[6] and a relatively large two-photon absorption (2PA) peak for C_{60} in toluene solution,[7] to our knowledge, it remains rare on the study of optical responsiveness of C_{60} derivatives to multiphoton absorption (MPA) processes in the near-infrared (>750 nm) region.

Concurrently, many molecular-design strategies have been successfully utilized to enhance two-photon absorption cross sections.[8] Most of these approaches have entailed molecular arrangement of chromophoric components in a linear,[9a] multibranched,[9b] octupolar[9e,10] oligomeric,[9c] or dendritic[9d,f] assembly pattern. That prompted us to commence investigation based on the structural design concept of merging RSA and 2PA synergistically in a molecular fullerenyl monoadduct system[11] with possible further extensions into the starburst structure of fullerenyl multiadducts. The main advantage envisioned for the success of this approach arises from the gain of a RSA state via a two-photon process using approximately half of the photonic energy required for a single-photon excitation. Combined MPA−RSA systems should also allow us to better understand the characteristics (rates, quantum efficiency, etc.) associated with excited states pumped by a two- or three-photon process. In this paper, we report the results that can be correlated by time-dependent nonlinear optical responses of diphenylaminofluorene-C_{60} conjugates upon collective simultaneous multiphoton and reverse saturable absorptions during either nanosecond laser flash photolysis or a femtosecond pump−probe experiment.

Experimental Section

General. Fluorene was purchased from Aldrich Chemicals. All other chemicals were purchased from Acros Ltd. A C_{60} sample in a purity of 99.5% was used. Further purification of C_{60} was made by thin-layer chromatography (TLC, SiO_2, toluene). Toluene and benzene were dried and distilled over sodium. ^{1}H NMR and ^{13}C NMR spectra were recorded on either a Bruker Spectrospin-400 or Bruker AC-300 spectrometer. Mass spectroscopic studies were performed by the use of positive ion fast atom bombardment (FAB^+) technique with a direct probe on a JEOL SX-102A mass spectrometer. Infrared spectra were recorded as KBr pellets on a Nicolet 750 series Fourier transform infrared (FT-IR) spectrometer.

Synthesis of 7-α-Bromoacetyl-9,9-di(3,5,5-trimethylhexyl)-2-diphenylaminofluorene 4, BrDPAF-C_9. A modified procedure was applied.[11b] To a suspension of aluminum chloride (2.0 g, 15.2 mmol) in 1,2-dichloroethane (30 mL) at 0 °C was added a solution of 9,9-di(3,5,5-trimethylhexyl)-2-diphenylaminofluorene (3.17 g, 5.4 mmol) in 1,2-dichloroethane (30 mL). It was then added by α-bromoacetyl bromide (0.66 mL, 7.5 mmol) over 10 min while maintaining the temperature of reaction mixture between 0 and 10 °C. The mixture was warmed to ambient temperature and stirred for an additional 2.0 h. At the end of the reaction, it was quenched by slow addition of water (100 mL) while maintaining the temperature below 45 °C. The organic layer was separated and washed sequentially with dilute HCl (1.0 N, 50 mL) and water (50 mL × 2). The liquid was dried over sodium sulfate and concentrated in vacuo to afford the crude product as crystalline yellow solids. The solids were purified by column chromatography (silica gel) using hexane/EtOAc/9:1 as eluent. A chromatographic fraction corresponding to $R_f = 0.7$ on thin-layer chromatography (TLC, SiO_2, hexane/EtOAc/9:1 as eluent) was isolated to give 7-α-bromoacetyl- 9,9-di(3,5,5-trimethylhexyl)-2-diphenylaminofluorene **4** as a yellow viscous oil in 70% yield (2.9 g). Spectroscopic data of **4** were reported previously.[11b]

Synthesis of 7-(1,2-Dihydro-1,2-methanofullerene[60]-61-carbonyl)-9,9-di(3,5,5-trimethylhexyl)-2-diphenylaminofluorene Monoadduct 2, C_{60}(>DPAF-C_9), and Bisadduct, C_{60}(Methanocarbonyl-9,9-di(3,5,5-trimethylhexyl)-2-diphenylaminofluorene)$_2$ 3, C_{60}(>DPAF-C_9)$_2$. C_{60} (1.0 g, 1.38 mmol) and 7-bromoacetyl-9,9-di(3,5,5-trimethylhexyl)-2-diphenylaminofluorene (BrDPAF-C_9, 0.97 g, 1.38 mmol) were dissolved in toluene (700 mL) under an atmospheric pressure of nitrogen. To this mixture was added 1,8-diazabicyclo[5.4.0]undec-7-ene (DBU, 0.2 mL, 1.38 mmol), and the mixture was stirred at room temperature for a period of 5 h. At the end of stirring, suspended solids of the reaction mixture were filtered off and the filtrate was concentrated to a 10% volume. Methanol (100 mL) was then added to the liquid to cause precipitation of crude products, which were isolated by centrifugation. Resulting solids were a mixture of monoadduct **2** and bisadduct **3**. Further separation of **2** and **3** was made by column chromatography (silica gel) using a solvent mixture of hexane/toluene/3:2 as

(6) (a) Lamrani, M.; Hamasaki, R.; Mitsuishi, M.; Miyashita, T.; Yamamoto, Y. *Chem. Commun*. **2000**, 1595−1596. (b) Koudoumas, E.; Konstantaki, M.; Mavromanolakis, A.; Couris, S.; Fanti, M.; Zerbetto, F.; Kordatos, K.; Prato, M. *Chem.—Eur. J*. **2003**, *9*, 1529−1534.

(7) (a) A relatively large 2PA peak (with fs cross-section of $\sim 80 \times 10^{-50}$ cm^4 s) was observed at 314 nm (but not at 930 nm) for a C_{60}/toluene solution by a nondegenerate two-photon spectroscopic study; see Yamaguchi, S.; Tahara, T. *Chem. Phys. Lett.* **2004**, *390*, 136−139. (b) Theoretical and experimental results also indicated the possibility of 2PA peak around 520 nm; see Zhou, X.; Ren, A.-M.; Feng, J.-K. *THEOCHEM* **2004**, *680*, 237−242 and references therein. (c) Sahraoui, B.; Kityk, I. V.; Bielieninik, J.; Hudhomme, P.; Gorgues, A. *Mater. Lett.* **1999**, *41*, 164−172.

(8) (a) Albota, M.; Beljonne, D.; Bredas, J. L.; Ehrlich, J. E.; Fu, J. Y.; Heikal, A. A.; Hess, S. E.; Kogej, T.; Levin, M. D.; Marder, S. R.; McCord-Maughon, D.; Perry, J. W.; Rockel, H.; Rumi, M.; Subramaniam, G.; Webb, W. W.; Wu, X. L.; Xu, C. *Science (Washington, D. C.)* **1998**, *281*, 1653−1656. (b) Reinhardt, B. A.; Brott, L. L.; Clarson, S. J.; Dillard, A. G.; Bhatt, J. C.; Kannan, R.; Yuan, L.; He, G. S.; Prasad, P. N. *Chem. Mater*. **1998**, *10*, 1863−1874. (c) Lin, T. C.; Chung, S. J.; Kim, K. S.; Wang, X.; He, G. S.; Swiatkiewicz, J.; Pudavar, H. E.; Prasad, P. N. *Adv. Polym. Sci.* **2003**, *161*, 157. (d) Katan, C.; Terenziani, F.; Mongin, O.; Werts, M. H. V.; Porres, L.; Pons, T.; Mertz, J.; Tretiak, S.; Blanchard-Desce, M. *J. Phys. Chem. A* **2005**, *109*, 3024−3037. (e) Woo, H. Y.; Hong, J. W.; Liu, B.; Mikhailovsky, A.; Korystov, D.; Bazan, G. C. *J. Am. Chem. Soc*. **2005**, *127*, 820−821. (f) Zhao, Y.; Shirai, Y.; Slepkov, A. D.; Cheng, L.; Alemany, L. B.; Sasaki, T.; Hegmann, F. A.; Tour, J. M. *Chem.—Eur. J*. **2005**, *11*, 3643−3658.

(9) (a) Rumi, M.; Ehrlich, J. E.; Heikal, A. A.; Perry, J. W.; Barlow, S.; Hu, Z.; McCord-Maughon, D.; Parker, T. C.; Rockel, H.; Thayumanavan, S.; Marder, S. R.; Beljonne, D.; Bredas, J. L. *J. Am. Chem. Soc.* **2000**, *122*, 9500. (b) Abbotto, A.; Beverina, L.; Bozio, R.; Facchetti, A.; Ferrante, C.; Pagani, G. A.; Pedron, D.; Signorini, R. *Chem. Commun.* **2003**, 2144−2145. (c) Belfield, K. D.; Morales, A. R.; Hales, J. M.; Hagan, D. J.; Van Stryland, E. W.; Chapela, V. M.; Percino, J. *Chem. Mater*. **2004**, *16*, 2267. (d) Drobizhev, M.; Karotki, A.; Rebane, A.; Spangler, C. W. *Opt. Lett*. **2001**, *26*, 1081. (e) Porres, L.; Mongin, O.; Katan, C.; Charlot, M.; Pons, T.; Mertz, J.; Blanchard-Desce, M. *Org. Lett.* **2004**, *6*, 47. (f) Hua, J. L.; Li, B. M.; Fan S.; Ding, F.; Qian, S. X.; Tian, H. *Polymer* **2004**, *45*, 7143−7149.

(10) Kannan, R.; He, G. S.; Lin, T.-C.; Prasad, P. N.; Vaia, R. A.; Tan, L.-S. *Chem. Mater*. **2004**, *16*, 185−194.

(11) (a) Chiang, L. Y.; Padmawar, P. A.; Canteenwala, T.; Tan, L. S.; He, G. S.; Kannan, R.; Vaia, R.; Lin, T. C.; Zheng, Q.; Prasad, P. N. *Chem. Commun*. **2002**, 1854−1855. (b) Padmawar, P. A.; Canteenwala, T.; Tan, L.-S.; Chiang, L. Y. *J. Mater. Chem*. **2006**, *16*, 1366−1378.

eluent. The first chromatographic band at $R_f = 0.45$ on the thin-layer chromatographic (TLC, SiO_2) plate using hexane/toluene/3:2 as eluent afforded the monoadduct **2**, 7-(1,2-dihydro-1,2-methanofullerene[60]-61-carbonyl)-9,9-di(3,5,5-trimethylhexyl)-2-diphenylaminofluorene, as greenish brown solids (960 mg, 70% yield based on recovered C_{60}). The second chromatographic band corresponding to $R_f = 0.25$ on TLC gave the bisadduct **3**, C_{60}(methanocarbonyl-9,9-di(3,5,5-trimethylhexyl)-2-diphenylaminofluorene)$_2$, C_{60}(>DPAF-C_9)$_2$, as brownish solids in a yield of 14% (190 mg). Spectroscopic data of **2** and **3** were reported previously.[11b]

Steady-State Optical Measurements. Steady-state UV−vis absorption spectra were recorded either on a Cary 500 spectrophotometer or on a Hitachi U-3410 UV spectrometer. Fluorescence emission spectra were recorded using either a Perkin-Elmer model LS 50B spectrofluorometer or a FLUOROLOG (ISA Instruments) spectrofluorometer.

Time-Resolved Single-Photon Counting and Femtosecond and Nanosecond Transient Absorption Measurements. Time-correlated single-photon counting technique (Edinburgh Instruments OB 920 spectrometer) was utilized to determine the lifetime of singlet states. During the experiment, the sample was photoexcited at 400 nm using a 70-ps laser diode. Subsequent photoemission was detected and recorded on a cooled microchannel plate PMT. The data were analyzed using a reconvolution software package provided by Edinburgh Instruments.

Nanosecond transient absorption measurements were carried out using the third harmonic (355 nm) of a *Q*-switched Nd:YAG laser (Quantel Brilliant, pulse width ca. 5.0 ns). Pulse fluences of up to 8.0 mJ cm^{-2} at the excitation wavelength were typically used. A detailed description of the laser flash photolysis apparatus was described previously.[12] Ultrafast pump−probe transient absorption measurements were performed using a 100 fs pulse (1.0 mJ) at 800 nm with a 1 kHz repetition rate, obtained from a diode-pumped, Ti:sapphire regenerative amplifier (Spectra Physics Hurricane). The 800 nm beam was split and focused into the sample. The split beam was delayed and then focused into a sapphire plate to generate a white light continuum. The white light was then overlapped with the pump beam in a 2-mm quartz cuvette and coupled into a charge-coupled device (CCD) detector. Details of the ultrafast system are described elsewhere.[13]

Results and Discussion

Combinative arrangement of reverse saturable absorbing C_{60} cage and 2PA-active diphenylaminofluorene (DPAF) moieties into one integrated chromophore compound constitutes the structural backbone of our approach for the synthesis of multiphoton absorptive materials (see Scheme 1). This molecular design is following the generic "C_{60}-*keto*-donor" structural motif, where C_{60} serves as an acceptor (A). In principle, direct conjugation of the donor (D) to C_{60} cage is desirable for enhancing orbital coupling and π-electron interactions between fullerene cage and aromatic donor addends. However, functionalization on fullerenyl double bonds often accompanies the corresponding change of sp^2 to sp^3 carbons, bridging each addend group to the rest of π-conjugation at the cage surface. To circumvent this inevitable setback, a through-space π-orbital overlapping mechanism was applied to establish the effective "periconjugation" path for possible electron interactions.[14] Such an approach requires selective placement of aromatic chromophore attachments immediately on fullerenyl sp^3 carbons. A close example was given by a covalently linked D−A conjugate C_{60}(>DPAF-C_2) **1**, 7-(1,2-dihydro-1,2-methanofullerene[60]-61-carbonyl)-9,9-diethyl-2-diphenylaminofluorene, demonstrated recently by our group.[11] In this structure, a highly fluorescent diethyl-2-diphenylaminofluorene (DPAF-C_2) donor moiety was found to be located in a close proximity of only ~2.8 Å to the C_{60} cage via a carbonyl group, as determined by X-ray structural analyses[11] and as shown in Figure 1. The close contact may contribute to enhancement of orbital and electronic interactions between π-electrons of both *keto*-DPAF and fullerene subunits and be reasoned for its measured large molecular 2PA cross

Scheme 1. Synthesis of the Monoadduct C_{60}(>DPAF-C_9) and the Corresponding Bisadduct C_{60}(>DPAF-C_9)$_2$; Reagents and Synthetic Conditions: *i*, C_{60}, DBU, Toluene, r.t. 5 h.

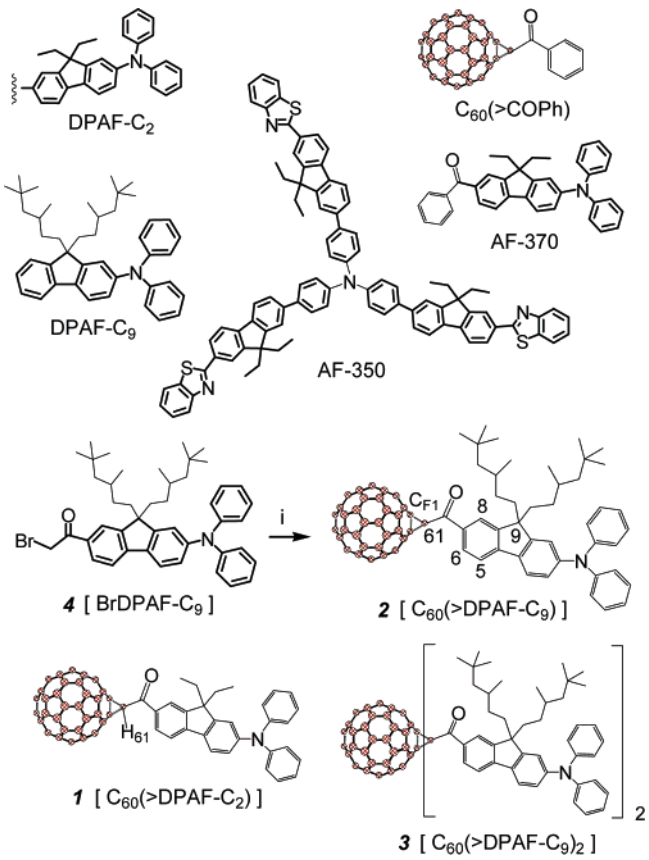

(12) Rogers, J. E.; Cooper, T. M.; Fleitz, P. A.; Glass, D. J.; McLean, D. G. *J. Phys. Chem. A* **2002**, *106*, 10108.

(13) Rogers, J. E.; Slagle, J. E.; McLean, D. G.; Sutherland, R. L.; Sankaran, B.; Kannan, R.; Tan, L. S.; Fleitz, P. A. *J. Phys. Chem. A* **2004**, *108*, 5514.

(14) (a) Wudl, F.; Sukuki, T.; Prato, M. *Synth. Met*. **1993**, *59*, 297−305. (b) Knight, B.; Martin, N.; Ohno, T.; Orti, E.; Rovira, C.; Veciana, J.; Vidal-Gancedo, J.; Viruela, P.; Viruela, R.; Wudl, F. *J. Am. Chem. Soc*. **1997**, *119*, 9871−9882. (c) Hamasaki, R.; Ito, M.; Lamrani, M.; Mitsuishi, M.; Miyashita, T.; Yamamoto, Y. *J. Mater. Chem*. **2003**, *13*, 21−26.

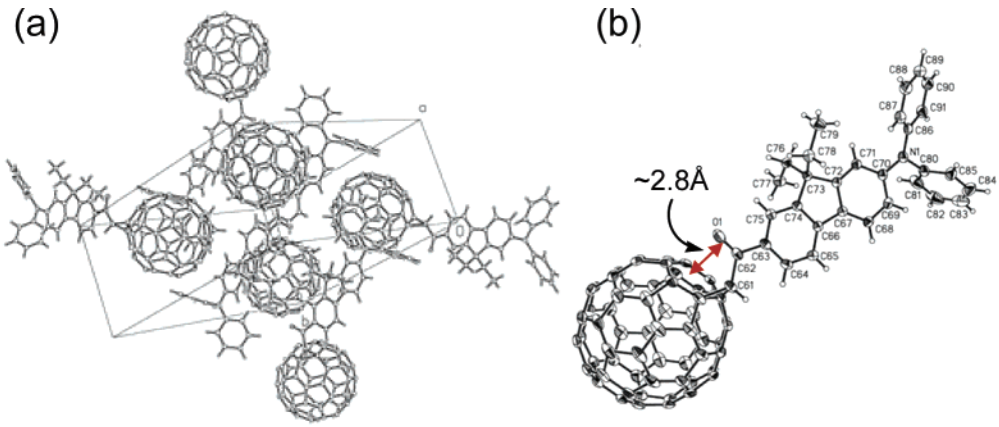

Figure 1. (a) Molecular packing of C_{60}(>DPAF-C_2) **1** in a monoclinic unit cell system with a space group of $P2_1/n$ determined by X-ray single-crystal structural analysis as reported,[11] and (b) ORTEP view showing the closest distance between C_{60} and *keto*-DPAF-C_2.

sections (σ_2') as 196×10^{-48} cm^4 s (or 1.96×10^4 GM in nanosecond region) in CS_2.

We further proposed that the spherical shape of a C_{60} cage should allow it to serve as a central molecular core for building multiple 2PA-ative chromophores in a starburst 3D-structure leading to A−$(D)_x$ conjugates, such as fullerenyl multiadducts C_{60}(>DPAF-$C_n)_x$. Several interconnected DPAFs in a branched structure on C_{60} provide a means to increase MPA cross sections and decrease the tendency of molecular close-packing. However, at a low degree of branching on C_{60}, such as the structure of fullerenyl monoadduct and bisadduct, intermolecular aggregation problems may still persist that reduce overall MPA efficiency. It is worthwhile to note that strong hydrophobic interactions among unfunctionalized half-spheres of the monoadduct cage lead to its high coalescence tendency, even in the presence of covalently attached DPAF-C_2. Molecular aggregation of fullerene cages induces intermolecular interactions between the excited singlet state of C_{60}(>DPAF-C_2) and the nearby fullerene moiety in its ground state. The phenomenon competes with the intersystem crossing process that decreases the population of the excited triplet state. Therefore, we incorporated alkyl side chains (C_n) with increasing steric hindrance and the chain size at close proximity of the rigid, planar aromatic DPAF moiety to prohibit effective packing and long-range molecular ordering of C_{60}-DPAF conjugates in the solid phase. Modification also increases significantly the solubility of resulting chromophore conjugates and makes tight aromatic interactions more difficult with each other in dense solution. Enhanced solubility facilitates the preparation of a highly concentrated solution for 2PA measurements. Specifically, we applied 3,5,5-trimethylhexyl (−C_9) groups to replace ethyl (−C_2) groups of **1**, giving new assemblies of C_{60}(>DPAF-$C_9)_x$ ($x = 1$ or 2). The steric effect induced by C_9 groups may allow us to analyze the influence of chromophore ordering on the value of two-photon absorption cross sections and to study its nonlinear optical responses in nanosecond and femtosecond regions.

Synthesis and Characterization of Multiphoton Absorbing C_{60}(>DPAF-$C_n)_x$. Incorporation of two bulky 3,5,5-trimethylhexyl side-chains on one diphenylaminofluorene (DPAF) ring is best carried out at the C_9 position of DPAF because of the readily available synthetic procedure.[11] Attachment of the resulting dialkylated DPAF donor component onto the C_{60} framework can be made via a α-cyclopropylketo linker leading to a C_{60}-*keto*-DPAF structure that brings the chromophore into the closest vicinity of a fullerenyl π-electron system. Retroelucidatation on the synthetic pathway of such fullerene derivatives leads to the use of 7-bromoacetyl-9,9-di(3,5,5-trimethylhexyl)-2-diphenylaminofluorene **4** (BrDPAF-C_9) as a corresponding key reactive precursor intermediate. Experimentally, the intermediate **4** was obtained in a roughly 65% yield by the reaction of 9,9-di(3,5,5-trimethylhexyl)-2-diphenylaminofluorene with α-bromoacetyl bromide (1.2 equiv) via Friedel−Crafts acylation in the presence of aluminum chloride (1.1 equiv) at 0 °C to ambient temperature for 4.0 h. Subsequent Bingel cyclopropanation reaction[15] of **4** with C_{60} in the presence of 1,8-diazabicyclo[5.4.0]undec-7-ene (DBU, 1.0 equiv) at ambient temperature for 5.0 h afforded the monoadduct C_{60}(>DPAF-C_9) **2** as greenish brown solids in 70% yield (based on recovered C_{60}). This reaction was also accompanied by the corresponding bisadduct C_{60}(>DPAF-$C_9)_2$ **3** as brownish solids in roughly 10% yield. Separation and purification of **2** ($R_f = 0.6$) and **3** ($R_f = 0.3$) was carried out on thin-layer chromatography (TLC, SiO_2) using a solvent mixture of hexane/toluene/3:2 as eluent.

Positive FAB mass spectra (FAB$^+$-MS) of both **2** and **3** displayed clearly a group of molecular ion (M^+) peaks with the peak maximum at *m*/*z* 1346 and 1971, respectively, in good agreement with their corresponding molecular mass. By using the spectrum of DPAF-C_9 in Figure 2a as the reference for comparison, we found that ^{13}C NMR spectrum of **2** (Figure 2c) fits well with its molecular structure, showing retention of all di(3,5,5-trimethylhexyl)diphenylaminofluorenyl carbon peaks in corresponding aliphatic and aromatic carbon regions. Since the molecular structure of C_{60}(>DPAF-C_2) was previously determined unequivocally by an X-ray single-crystal structural study,[11] its aromatic carbon peak pattern and the values of chemical shift, as shown in Figure 2b, can be utilized to assist the peak assignment of **2**. In fact, close spectral resemblance between parts b and c of Figure 2 with respect to the fullerenyl carbon (C_F) pattern and the relative intensity of peaks in the range

(15) Bingel, C. *Chem. Ber.* **1993**, *126*, 1957.

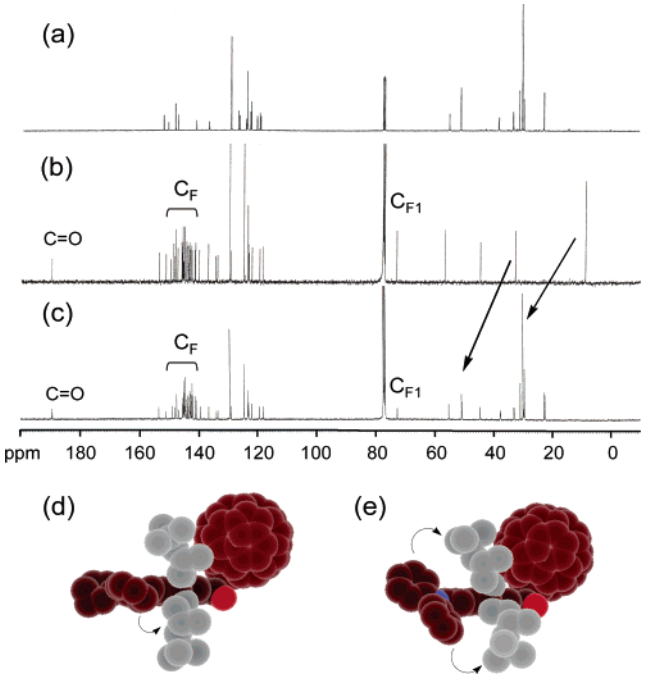

Figure 2. ^{13}C NMR spectra of (a) DPAF-C_9, (b) C_{60}(>DPAF-C_2) **1**, and (c) C_{60}(>DPAF-C_9) **2** showing a close resemblance in a chemical-shift pattern of fullerenyl carbon (C_F) peaks. Schematic molecular simulation of alkyl steric hindrance on diphenylamino moiety of **2** showed high repulsion between phenyl groups and alkyl side-chains in (d), and reduced hindrance in (e) when the DPAF group was bent slightly away from the fluorene plane.

of δ 135−150 provided a convincing proof of high similarity in the overall structure between monoadducts **1** and **2**. Consequently, a total of 29 fullerenyl carbon peaks distributed in this region reveals a C_2 symmetry for 58 sp^2 C_F carbons of the C_{60} cage. An additional carbon peak at δ 189 was assigned to the chemical shift of a carbonyl carbon. Chemical shifts of two remaining fullerenyl sp^3 carbons C_{F1} and C_{F2} were found to be identical at δ 73. Apparent large downfield shifts of alkyl carbon peaks over 20−30 ppm, as indicated by the arrows, were observed going from ethyl groups of **1** to 3,5,5-trimethylhexyl groups of **2**. It may be related to the intramolecular steric hindrance effect of bulky alkyl side-chains. On the basis of schematic molecular 3D models shown in parts d and e of Figure 2, two 3,5,5-trimethylhexyl groups of **2** seem to be capable of forcing the adjacent diphenylamino group to twist slightly away from the plane of fluorene-ring moiety in order to reduce the hindrance. This preferred steric configuration might have a pronounced effect on the nature of intermolecular aggregation as the solution concentration of C_{60}(>DPAF-C_9) increases largely.

Heteronuclear multiple quantum coherence (HMQC) technique used in $^1H-^{13}C$ NMR measurement provides the correlation between proton and carbon nuclei while recording proton peaks. This type of 2D-resolved NMR experiment allows us to correlate the peak of C_{61} precisely to the peak of H_{61} in chemical shift and all cross-peaks between other fluorenyl protons and carbons for further confirmation of NMR peak assignments. As a result of comparison between Figures 2c and 3, all nonprotonated fullerenyl carbon peaks were substantiated with many of the fluorenyl carbon peaks assigned, including those of C_{F1} at δ 72.6, nonprotonated

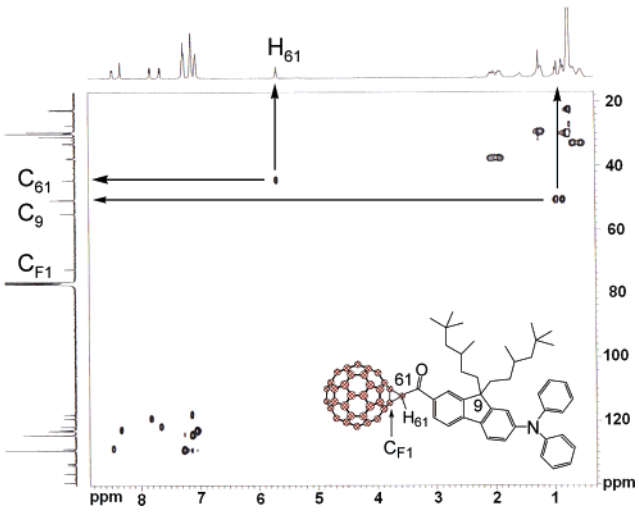

Figure 3. $^1H-^{13}C$ 2D NMR spectrum of C_{60}(>DPAF-C_9) **2** using HMQC technique showing correlation of the carbon peak to the peak of proton bound on the same carbon.

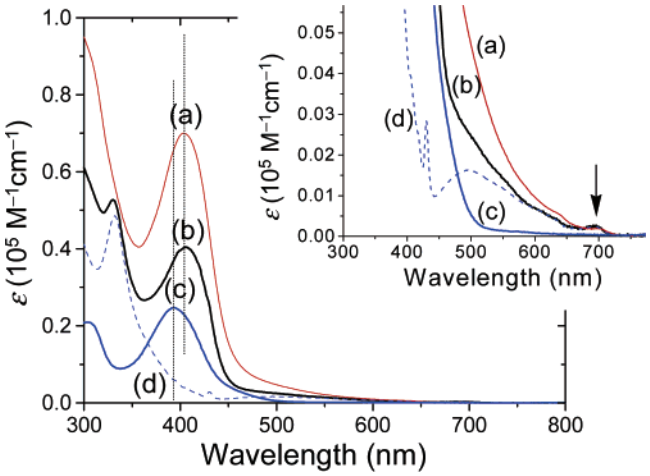

Figure 4. Steady-state UV−vis absorption spectra of (a) C_{60}(>DPAF-C_9)$_2$ **3**, (b) C_{60}(>DPAF-C_9) **2**, (c) (BrDPAF-C_9) **4**, and (d) C_{60}(>COPh) in benzene.

C_9 at δ 55.2, the second methylene carbon next to C_9 at δ 50.9, and C_{61} at δ 44.6. These data are consistent with the structure of C_{60}(>DPAF-C_9), as depicted in Figure 3. The influence of fullerenyl current through space was noticed by a strong deshielding effect on the α-proton H_{61} of cyclopropylketo group and some fluorenyl protons of **1** and **2**. For example, the effect caused chemical shifts of H_{61} and fluorene protons at C_5, C_6, and C_8 of **2** to downshift to δ 5.69, 7.83, 8.48, and 8.32, respectively, with roughly a 0.2−0.5 ppm shift from those of phenyl protons at C_5, C_6, and C_8 of **4** (BrDPAF−C_9) at δ 7.65, 7.95, and 7.92, respectively.

Steady-State Single-Photon Absorbance Measurement. Steady-state UV−vis absorption spectra of C_{60}(>DPAF-C_9) **2**, C_{60}(>DPAF-C_9)$_2$ **3**, BrDPAF-C_9 **4**, and C_{60}(>COPh) were recorded in air-saturated benzene. Spectral features of both C_{60}(>DPAF-C_9) (Figure 4b) and C_{60}(>DPAF-C_9)$_2$ (Figure 4a) arise from two optical bands centered at 310−326 and 406−410 nm, corresponding to the absorption of DPAF and C_{60} cage moieties, respectively. Absorption of these two individual moieties were independently confirmed by the equivalent model compounds C_{60}(>COPh) and BrDPAF-C_9, showing optical bands at 328 and 407 nm, respectively.

Absorption peak intensity of C_{60}(>DPAF-C_9) in Figure 4b is not the simple sum of parts c and d of Figure 4 of model compounds, indicating certain interactions are present between DPAF and C_{60} moieties that influence its optical absorption characteristics. In the case of C_{60}(>DPAF-C_9)$_2$, the absorption band at 406 nm is nearly twice as large in intensity as that of C_{60}(>DPAF-C_9), and is, thus, in good agreement with its composition consisting of two DPAF arms. Most importantly, an additional weak but characteristic long wavelength absorption band of the C_{60} cage centered at roughly 690 nm was detected for all fullerene-containing monoadduct **2**, bisaduct **3**, and C_{60}(>COPh), as shown in the insert of Figure 4, giving the confirmation of **2** and **3** as C_{60}-conjugated structures with a similar ground to singlet excited-state energy gap.

Nanosecond Multiphoton Absorption Cross-Section Measurements. Determination of effective two-photon absorption cross-section values in the nanosecond region was made using the photoexcitation wavelength of 800 nm. This near-infrared wavelength fits well within a spectral transparent window of 800−1100 nm in mammalian tissue[16] that should enhance effective light penetration depth into the tissue and cells for the practice of photodynamic therapy (PDT). 2PA evaluation on C_{60}(>DPAF-C_9) and C_{60}(>DPAF-C_9)$_2$ samples was performed in CS_2 at the concentrations of 0.02 and 0.01 M, respectively, using the standard nonlinear transmission (NLT) measurement method.[17] It is worthwhile to point out that this simple and direct NLT method for the measurement is operated based on the assumption of two-photon absorption being the predominant process triggering observed intensity-dependent nonlinear absorptions. However, as many researchers have indicated,[18] strong 2PA process may considerably increase molecular populations in excited states of the molecule that gives possible initiation of a secondary process, i.e., cascaded single-photon absorptions from excited states, and create additional contribution to the observed nonlinear absorption value. This additional component makes accurate counting of the excited-state absorption more difficult following two-photon pumping. Therefore, the values of effective 2PA cross sections obtained in nanosecond measurements are invariably much greater than intrinsic ones that entail our use of subpicosecond laser pulses in the second measurement for confirmation. Nevertheless, by using the same structural moieties for the construction of various C_{60}-DPAF conjugates under systematic variation of only one certain component in each series, we expect to keep electronic characteristics and excited-state properties of both individual C_{60} and DPAF moieties consistent among these derivatives for comparison. The approach makes the measured effective cross-section data semiquantitatively useful in terms of the trend in the change of relative 2PA absorptions upon the well-defined structural modification. Therefore, a qualitative correlation of the steric effect of peripheral alkyl groups to the variation of NLT data obtained in this work should be valid.

Table 1. Measurement of 2PA Cross Sections ($\sigma_2' = h\nu\sigma_2$) of 1, 2, and 3 Using Laser Pulses Working at Either 775 nm with ~160 fs Duration or 800 nm with ~8 ns Duration (The Semiquantitative Value of the Latter is Indicated in Parentheses for Trend Comparison)[a]

dye/solvent[b]	λ_{max}[c]/ nm	σ_2 (10^{-20} cm^4/GW)	σ_2' (10^{-48} cm^4 s)
AF-370/CS_2	389	0.115 (23)	0.285 (57)
AF-350/THF	400	0.530 (112)	1.32 (278)
C_{60}(>DPAF-C_2) **1**/CS_2	408	(79)	(196)
C_{60}(>DPAF-C_9) **2**/CS_2	406	0.123 (102)	0.306 (251)
C_{60}(>DPAF-C_9)$_2$ **3**/CS_2[d]	404	0.332 (251)	0.824 (622)

[a] Experimental uncertainty ±15%. [b] Concentration of 0.02 M. [c] Linear absorption. [d] Concentration of 0.01 M.

To further support such a correlation attempt, intrinsic 2PA cross sections of these chromophores in ~160 fs duration were also determined with Z-scan upon 2PA excitation at 775 nm besides the nanosecond measurement in ~8 ns duration at 800 nm. As a result, cross-reference of 2PA cross-section values among DPAF-derived fullerene derivatives **1**−**3** and pertinent AFX chromophores was summarized in Table 1. A trend was observed of largely increased 2PA cross sections in four folds going from linearly conjugated dipolar AF-370 to cross-conjugated octupolar AF-350 structure, indicating the importance of structural branching in enhancing the 2PA value and nonlinear optical behavior in addition to the degree of π-delocalization throughout the entire molecular structure.[10] In this regard, C_{60}(>DPAF-C_9)$_2$ bisadduct can be considered as the branched structure of the corresponding linear monoadduct analogous C_{60}(>DPAF-C_9). Owing to a relatively smaller C_{60} cage size than DPAF-C_9 arms, the steric hindrance tends to separate two DPAF addends at a certain distance on the cage surface that results in a preferred quadrupolar arrangement for branched bisadducts **3**.

By replacing the phenyl group of AF-370 by a methano-[60]fullerene cage (C_{60}>) to the structure of C_{60}(>DPAF-C_2) **1**, a large increase of the effective 2PA cross-section value by more than 3-fold to 196×10^{-48} cm^4 s (or 1.96×10^4 GM) was measured in CS_2. Since C_{60} was reported to be 2PA active only in the UV−visible region and inactive in the near-IR region,[7] potential direct 2PA contribution from C_{60} moiety of **1** alone at 800 nm could be ruled out. Therefore, observed simultaneous two-photon absorption enhancement arises mainly from the conjugated DPAF chromophore moiety located on the spherical surface of C_{60} monoadducts **1** and **2**. Bonding a DPAF donor onto a C_{60} acceptor in a close distance promotes π-electron polarizability along the orbital of resulting conjugated D−A molecules. That may be one of the reasons for largely increased two-photon absorption.

Interestingly, as the steric hindrance of the alkyl side chain increases by replacing both ethyl groups of **1** with 3,5,5-trimethylhexyl groups, the resulting compounds C_{60}(>DPAF-

(16) (a) Fisher, W. G.; Partridge, W. P., Jr.; Dees, C.; Wachter, E. A. *Photochem. Photobiol.* **1997**, *66*, 141−155. (b) Bhawalkar, J. D.; Kumar, N. D.; Zhao, C. F.; Prasad, P. N. *J. Clin. Laser, Med. Surg.* **1997**, *15*, 201−204.

(17) He, G. S.; Xu, G. C.; Prasad, P. N.; Reinhardt, B. A.; Bhatt, J. C.; McKellar, R.; Dillard, A. G. *Opt. Lett.* **1995**, *20*, 435.

(18) (a) Qiu, P.; Penzkofer, A. *Appl. Phys. B* **1989**, *48*, 115. (b) Prokhorenko, V. T.; Tikhonov, E. A.; Shpak, M. T. *Kvantovaya Elektron (Moscow)* **1981**, *8*, 229. (c) Foucault, B.; Hermann, J. P. *Opt. Commun.* **1975**, *15*, 412. (d) Kleischmidt, J.; Torpatschow, P. *Exp. Technol. Phys.* **1975**, *23*, 17. (e) Brunner, W.; Duerr, H.; Close, E.; Paul, H. *Kvantovaya Elektron (Moscow)* **1975**, *2*, 832. (f) Bergman, A.; Jortner, J. *Chem. Phys. Lett.* **1974**, *26*, 323. (g) Rapp, W.; Gronau, B. *Chem. Phys. Lett.* **1971**, *8*, 529. (h) Topp, M. R.; Rentepis, P. M. *Phys. Rev.* **1971**, *A3*, 358.

C_9) and C_{60}(>DPAF-C_9)$_2$ in CS_2 manifest equivalent or even larger 2PA cross sections in the nanosecond region to 251 (or 2.51×10^4 GM) and 622×10^{-48} cm^4 s (or 6.22×10^4 GM), respectively, in comparison with those of AF-350 in the same wavelength range measured. The latter value was found to be the *largest* among AFX chromophores and C_{60}-DPAF compounds. On the basis of 2PA measurements in the femtosecond region upon excitation at 775 nm, the σ_2' value of 0.824×10^{-48} cm^4 s (or 82.4 GM) for the bisadduct **3** is higher than 0.306×10^{-48} cm^4 s (or 30.6 GM) for the monoadduct **2** in CS_2 with an increase of the value by 170%. However, these values are lower than 1.32×10^{-48} cm^4 s (or 132 GM) for AF-350. The ratio of cross-section values measured in ns- and fs-regions for AF-350 is roughly 187, whereas this ratio is 829 and 756 for **2** and **3**, respectively. A difference in the trend of relative σ_2' values among C_{60}-DPAF conjugates and AF-350 in either the ns- or fs-region may be interpreted by the occurrence of additional excited-state absorption, following the initial 2PA transition, for apparently much greater cross-section values measured in the ns-region. In other words, it revealed more efficient absorption with longer excitation pulses of nanoseconds, while the same absorption was kinetically prohibited or nonactivated under shorter excitation pulses of subpicoseconds. Alternative rationale may be raised from the inherent optical nonlinear absorption characteristics of the C_{60} cage based on its large excited-state absorption value.[7] Remarkably, these arguments can be correlated plausibly by the cause of a different transient excited state of C_{60}(>DPAF-C_9) involved in either fs or ns time scale, as concluded from transient absorption measurements described below. Accordingly, in an initial ultrashort period of ~160 fs, DPAF moiety was proposed to be the main chromophore of **1**−**3** in response to photoexcitation, leading to formation of the corresponding singlet excited-state C_{60}(>^{1}DPAF-C_9*), whereas triplet excited state of the C_{60} cage moiety becomes the dominated transient state above a longer period of ~1.4 ns time scale. A similar argument can be made to the significantly higher σ_2' value of C_{60}(>DPAF-C_9)$_2$ measured at 8 ns time scale accompanied with a lower value in the 160 fs-region than those of AF-350 as indicative of a much larger contribution of the triplet excited state $^3C_{60}$*(>DPAF-C_9)$_2$ to observed enhancement of 2PA cross sections in the ns-region.

The values of three-photon absorption (3PA) coefficient (γ) and cross sections (σ_3) of **2** and **3** were collected by the direct nonlinear transmission method upon excitation at 1460 nm,[19] as summarized in Table 2. The data indicated 3PA cross sections of C_{60}(>DPAF-C_9) in a σ_3 value of 2.59×10^{-25} cm^6/GW^2 in CS_2 falling in a similar range as that of highly three-photon absorbing AF-350 (2.64×10^{-25} cm^6/GW^2) in THF and a diphenylaminostyryldialkylfluorene oxadiazole derivative, denoted as PRL-801.[19b] A 143% increase in the σ_3 value was evident as the structure of C_{60}-DPAF conjugates being changed from the monoadduct **2** to the bisadduct **3**. Significant enhancement of 3PA cross sections to 6.30×10^{-25} cm^6/GW^2 for **3** was correlated to the structural modification with sterically hindered alkyl components to the triad analogous C_{60}(>DPAF-C_9)$_2$. This σ_3 value was found to be the *highest* 3PA cross sections among AFX series and C_{60}-DPAF compounds in this study.

(19) (a) He, G. S.; Bhawalkar, J. D.; Prasad, P. N.; Reinhardt, B. A. *Opt. Lett*. **1995**, *20*, 1524. (b) He, G. S.; Prasad, P. N. *Proceedings SPIE Nonlinear Optical Transmission and Multiphoton Processes in Organics*; Yeates, A. T., Belfield, K. D., Kajzar, F., Lawson, C. M., Eds.; SPIE: Bellingham, WA, 2003; Vol. 5211, p 1.

Table 2. Measurement of 3PA Coefficient γ and Cross Sections σ_3 of 2 and 3 Using Laser Pulses of 1460 nm with ~160 fs Duration[a]

dye/solvent[b]	3PA coefficient γ (10^{-5} cm^3/GW^2)	σ_3 (10^{-25} cm^6/GW^2)
AF-350 /THF	0.318	2.64
PRL-801 /$CHCl_3$	0.333	2.76
C_{60}(>DPAF-C_9) **2**/CS_2	0.312	2.59
C_{60}(>DPAF-C_9)$_2$ **3**/CS_2[c]	0.380	6.30

[a] Experimental uncertainty ±15%. [b] Concentration: 0.02 M. [c] Concentration: 0.01 M.

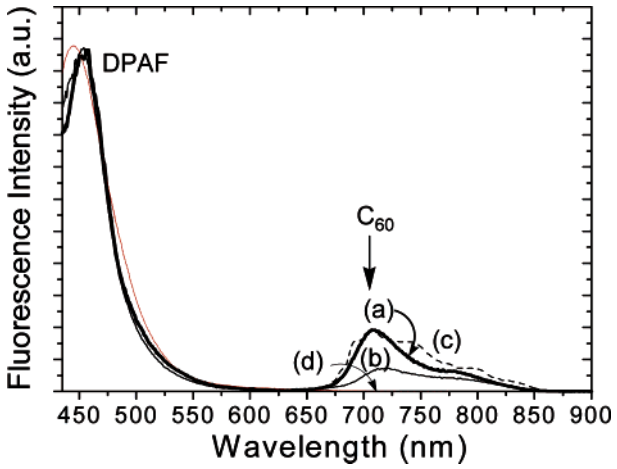

Figure 5. Fluorescence emission spectra of (a) C_{60}(>DPAF-C_9) **2**, (b) C_{60}-(>DPAF-C_9)$_2$ **3**, (c) C_{60}(>COPh), and (d) BrDPAF-C_9 upon excitation at 400 nm in air-saturated benzene. The spectrum is normalized at the 453 nm peak of DPAF emission for (a), (b), and (d).

Steady-State, Time-Resolved Emission, and Transient Absorption Measurements. Steady-state fluorescence spectra of **2**, **3**, **4**, and C_{60}(>COPh) in air-saturated benzene are shown in Figure 5. Upon photoexcitation at 400 nm, both C_{60}(>DPAF-C_9) and C_{60}(>DPAF-C_9)$_2$ resulted in dual emission peaks with one peak maximum centered at 453 nm and the other one centered at 708 (for **3**) or 719 (for **2**) nm with a tail extending to 825 nm. Using the emission spectra of model compounds C_{60}(>COPh) and BrDPAF-C_9 for comparison at the same excitation wavelength, we correlated the emission observed at 453 and 708−719 nm to the attribution of DPAF and C_{60} moieties, respectively. A much higher intensity of the band at 453 nm than that at 708 nm is indicative of spectrum predominance by the DPAF absorption at 400 nm excitation. A similar shape of tailing emission profiles at long wavelengths among C_{60}-containing **2**, **3**, and C_{60}(>COPh) revealed several emission mechanisms involved for fullerene monoadduct and bisadduct other than the emission source arising from the lowest excited singlet energy of $^1C_{60}$*(>DPAF-C_9) and $^1C_{60}$*(>DPAF-C_9)$_2$, estimated to be 1.75 and 1.72 eV, respectively, in benzene. There is a marked difference of the peak intensity ratio (I_{453}/I_{708}) between DPAF and C_{60} bands of **2** and **3** with a much higher value for the bisadduct **3**. It is indicative of increasing contribution from the emission of DPAF-C_9 moiety ap-

Table 3. Summary of Photophysical Properties of 2, 3, C_{60}(>COPh), and BrDPAF-C_9 4 in Benzene

	C_{60}(>DPAF-C_9)	C_{60}(>DPAF-C_9)$_2$	C_{60}(>COPh)	BrDPAF-C_9
Abs λ_{max}[a]	329, 406 nm	404 nm	332, 696 nm	394 nm
λ_{FLmax}[a]	453, 708 nm	452, 719 nm	708 nm	439 nm
E_s			1.77 eV	2.97 eV
τ_s[a]	1.49 ns (708 nm)	1.55 ns (719 nm)	1.35 ns (708 nm)	2.13 ns (445 nm)
Φ_{FL}[a]			0.0004	0.34
$(T_1-T_n)_{max}$[b]	720 nm	710 nm	720 nm	640 nm
τ_T[b]	42 μs	36 μs	39 μs	162 μs

[a] Air-saturated benzene. [b] Deoxygenated benzene (freeze pump thaw).

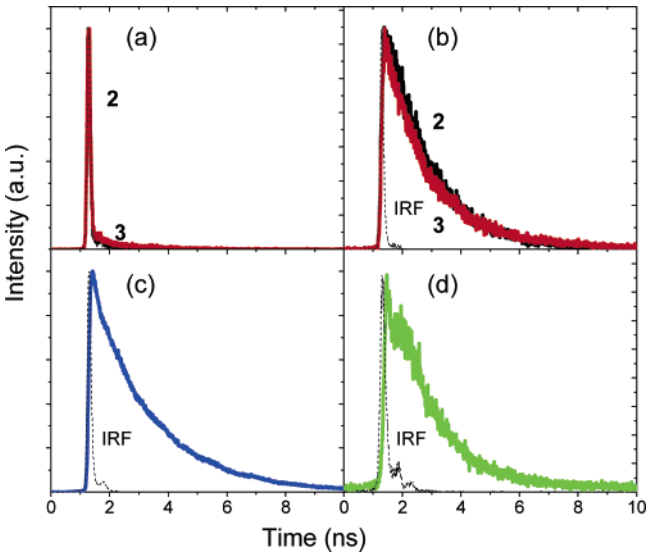

Figure 6. Time-correlated emission decay of (a) C_{60}(>DPAF-C_9) **2** and C_{60}(>DPAF-C_9)$_2$ **3**, both at 453 nm, (b) **2** at 708 nm and **3** at 719 nm, (c) BrDPAF-C_9 **4** at 439 nm, and (d) C_{60}(>COPh) at 708 nm in air-saturated benzene following excitation at 400 nm with a 70 ps diode laser. Lifetimes are given in Table 3.

proximately proportional to the number increase of fluorescent addend in **3**. That can be interpreted as low fluorescence quenching of multiple DPAF-C_9 subunits by the fullerene cage, via intramolecular energy transfer, in benzene.

Correlation of observed large 2PA cross sections of **2** and **3** to their transient characteristics in fs- and ns-regions was investigated using transient measurements in corresponding time scales with all photophysical properties summarized in Table 3. We first utilized time-correlated single-photon counting technique to measure the time-resolved kinetics of compounds **2** and **3** in air-saturated benzene to understand sequential photoresponsive events of both C_{60} and DPAF moieties. Recent reports have indicated strong solvent-dependent photoresponses of these fullerene derivatives, which concluded intramolecular energy transfer from the photoexcited DPAF moiety to the fullerene cage is the primary process in nonpolar solvents, such as benzene and toluene.[11b,20] Therefore, current studies may allow us to further substantiate this hypothesis. In this measurement, each sample was photoexcited at 400 nm by using a 70 ps diode laser with the results shown in Figure 6. At this wavelength, the absorption is dominated by DPAF moiety according to their steady-state UV−vis spectra (Figure 4). Subsequent fluorescence emission from the lowest excited singlet DPAF state at 440−455 nm was verified using the model compound BrDPAF-C_9 **4** in the same solvent. The spectrum (Figure 6c) displayed fluorescence λ_{FLmax} at 439 nm with 34% quantum efficiency (Φ_{FL}) and decay of the emission in a lifetime (τ_s) of 2.1 ns. Excitation of the C_{60} moiety is also possible at 400 nm, as demonstrated by the model compound C_{60}(>COPh) giving the fluorescence emission at 708 nm (Figure 6d), corresponding to the lowest excited singlet state $^1C_{60}$*(>COPh) energy, in a much lower intensity and quantum yield (Φ_{FL} = 0.04%) with a slightly faster decay rate (τ_s = 1.4 ns) than BrDPAF-C_9.

When detecting the emission intensity at 453 nm upon 70 ps pulse excitation of both chromophores C_{60}(>DPAF-C_9) and C_{60}(>DPAF-C_9)$_2$ at 400 nm, it was found to be nearly quenched within the instrument response function (IRF, 50 ps) with a small long-tail continuing in a lifetime of roughly 1.2 ns, as shown in Figure 6a. Interestingly, simultaneous detection probes of the emission of C_{60}(>DPAF-C_9) at 708 nm and C_{60}(>DPAF-C_9)$_2$ at 719 nm, both in Figure 6b, gave a biexponential emission decay profile with a fast growth (<50 ps) and long-lived emission lifetimes (τ_s) of 1.5 and 1.6 ns, respectively, in close resemblance to that of $^1C_{60}$*-(>COPh) in intensity and shape of the decay profile. These short lifetime values were of estimates that may not be reliable, owing to IRF limits. Nevertheless, based on high similarity of the emission intensity, τ_s, and the decay profile, we concluded that the fluorescence emission at 708−719 nm in **2** and **3** attributes to the C_{60} moiety.

Excited-State Properties of C_{60}(>DPAF-C_9) and C_{60}-(>DPAF-C_9)$_2$ in Measurements Using Either Nanosecond Laser Flash Photolysis or Two-Photon Pumping by Femtosecond Pulse Laser. To differentiate the observed fast DPAF fluorescence quenching (within 50 ps) by the C_{60} cage of **2** and **3**, mainly due to the occurrence of intramolecular energy transfer rather than competitive electron-transfer processes, we performed transient single-photon absorption spectrum measurements of **2** (9.2 μM), **3** (6.2 μM), and C_{60}-(>COPh) (9.9 μM) in deoxygenated benzene by nanosecond laser flash photolysis (>50 ns). The results were displayed in Figure 7b with the intensity of all peaks normalized at the peak maximum. A new absorption band of C_{60}(>DPAF-C_9) and C_{60}(>DPAF-C_9)$_2$ centered at 715 nm was observed immediately following nanosecond laser pulse at 355 nm. This band is nearly indistinguishable to that of C_{60}(>COPh) obtained under identical experimental conditions. Therefore, it was assigned to absorptions of the T_1-T_n transition of fullerene cage correlated to the related $^3C_{60}$* moiety.[21] The lack of detection of other possible characteristic transient

(20) Luo, H.; Fujitsuka, M.; Araki, Y.; Ito, O.; Padmawar, P.; Chiang, L. Y. *J. Phys. Chem. B* **2003**, *107*, 9312−9318.

(21) Komamine, S.; Fujitsuka, M.; Ito, O.; Morikawa, K.; Miyata, T.; Ohno, T. *J. Phys. Chem. A* **2000**, *104*, 11497.

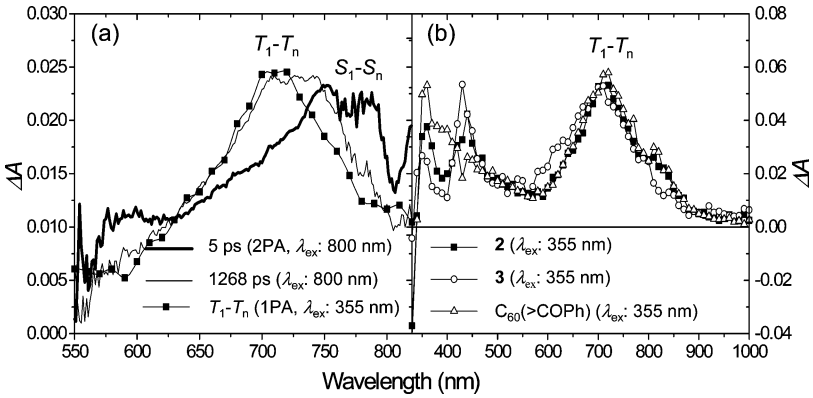

Figure 7. Transient absorption spectra of (a) C_{60}(>DPAF-C_9) **2** upon photoexcitation at 800 nm in air-saturated benzene (0.01 M) with a 100 fs pulse laser. It includes two spectra recorded at 5.0 and 1268 ps, following the femtosecond laser pulse, which overlaid with the nanosecond transient absorption spectrum of **2** upon excitation at 355 nm and normalized at the peak height to match with the ultrafast data. In (b) are the transient absorption spectra of **2**, **3**, and C_{60}(>COPh) normalized at the peak height following the nanosecond excitation in deoxygenated benzene.

absorption bands at 1000 nm for C_{60}^{-}• moiety and 840 nm for (DPAF-C_n)$^{+}$• moiety of radical ion-paired intermediates[20] C_{60}^{-}•[>(DPAF-C_n)$^{+}$•] excluded the involvement of intramolecular electron transfer from DPAF-C_9 to C_{60} cage during the nanosecond photoexcitation. Instead, it confirmed clearly ultrafast intramolecular energy transfer processes going from excited singlet C_{60}[^{1}(DPAF-C_9)*]$_x$ to the C_{60} cage, forming the corresponding transient excited triplet state intermediate $^{3}C_{60}$* (>DPAF-C_9)$_x$ (x = 1 or 2) in benzene in nanoseconds. Several peaks in the region of 350−500 nm were attributed to the absorption of different ground states among the samples.

Experimental attempts were made to detect time-resolved fluorescence of **2** and **3** upon photoexcitation with a 100 fs pulse at 800 nm, which is mainly effective for the DPAF moiety. Unfortunately, the intensity of fluorescence emission based on this two-photon absorption process was too weak to be detected, consistent with previous observation on a C_{60}-(>DPAF-C_2) sample excited by a nanosecond pulse laser at 800 nm.[11] By the fact that no emission from the DPAF moiety of **2** and **3** was recorded at 453 nm, we concluded full quenching of the fluorescence occurring under the event of two-photon absorption process.

Femtosecond pump−probe transient absorption spectra collected upon photoexcitation at 800 nm was utilized to understand the excited-state kinetics of C_{60}(>DPAF-C_9) in air-saturated benzene. The transient state was probed with a white light continuum generated using a sapphire plate, as previously described.[13] We found that the femtosecond data of **2** (Figure 7a) overlaid well with the T_1-T_n transient absorption profile (Figure 7b) of the $^{3}C_{60}$* moiety of **2** taken by the nanosecond laser flash photolysis measurement. At an extremely short time scale of ∼5 ps immediately after excitation by a 100 fs laser pulse, a new transient absorption spectral profile of **2** with the peak maxima centered at 740−780 nm was obtained, in close resemblance to the singlet excited-state absorbance of C_{60} reported previously.[22] Therefore, we assigned this band profile to the S_1-S_n transient absorption of the ^{1}(C_{60}>)* moiety of **2**. A subsequent spectrum collected at a longer time scale of 1268 ps after the laser pulse excitation showed a blue-shift of the peak, with the peak maxima located over the range of 700−750 nm. It nearly superimposes with that of the peak maxima at 690−725 nm obtained from nanosecond laser flash photolysis measurements and is attributed to the T_1-T_n transient absorption of triplet excited state ^{3}(C_{60}>)*. There was no evidence of absorbance attributed from the DPAF moiety or intramolecular electron transfer-derived intermediates.[20] The recorded energy-transfer process going from DPAF to the C_{60} cage was extremely efficient. In fact, this process occurred within the instrument response function, which is ∼130 fs. In summary, the longer time decay in this experiment was correlated with the singlet decay of ^{1}(C_{60}>)* state of **2** into the corresponding triplet ^{3}(C_{60}>)* state via an intersystem energy crossing with a lifetime of ∼1.4 ns. A similar energy-transfer process resulting in the triplet state formation of the fullerene cage in $^{3}C_{60}$*(>DPAF-C_2) was detected in toluene with a triplet excited-state lifetime of 33 μs.[20] Femtosecond transient absorption measurement also revealed ultrafast photoresponse within 10 ps immediately following 150-fs laser pulse excitation. A close linkage of DPAF-C_2 to the fullerene cage by a short separation distance of only 2.0−3.0 Å was proposed for this effective intramolecular photoprocess in an extremely short time scale.

Combination of both results from femtosecond pump−probe transient absorption experiments at 800 nm and nanosecond laser flash photolysis at 355 nm verified clearly the occurrence of two-photon excitation processes of **2** in air-saturated benzene and a subsequent efficient energy transfer from the two-photon pumped DPAF moiety to the C_{60} cage moiety. That allowed us to resolve early time kinetics for different processes involved during the two-photon pumping procedure on C_{60}(>DPAF-C_9), as illustrated in Scheme 2. We proposed that the initial two-photon energy absorption occurred primarily on the DPAF-C_9 moiety of **2**, leading to the formation of singlet excited-state C_{60}[^{1}(DPAF-C_9)*], as depicted in panel (a). Subsequent ultrafast intramolecular energy transfer from DPAF-C_9 moiety to the methanofullerene (C_{60}>) moiety took place within the instrument response function (130 fs) of pump−probe transient absorption experiments. Panel (b) shows intersystem crossing of the electron from the singlet $^{1}C_{60}$*(>DPAF-C_9) state to the

(22) Ebbesen, T. W.; Tanigaki, K.; Kuroshima, S. *Chem. Phys. Lett.* **1991**, *181*, 501.

Scheme 2. Proposed Potential Energy Diagram of C_{60}(>DPAF-C_9) in Ultrafast Kinetic Processes upon Femtosecond Two-Photon Absorption-Based Excitation at 800 nm in Benzene

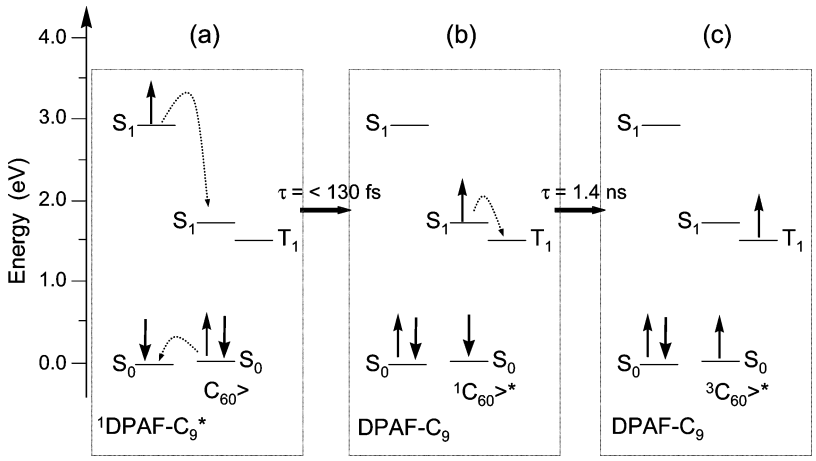

lowest triplet excited state $^3C_{60}$*(>DPAF-C_9) that occurs on a time scale of 1.4 ns.

Conclusions

Structural combination of diphenylaminofluorene and C_{60} provides an important mechanism in enhancing multiphoton responses. To our knowledge, C_{60}(>DPAF-C_9) and C_{60}-(>DPAF-C_9)$_2$ are the first examples of C_{60}-containing compounds showing high three-photon absorption activities. The compound C_{60}(>DPAF-C_9)$_2$ exhibits 2PA and 3PA cross sections in the values of 0.824×10^{-48} cm^4 s (or 82.4 GM) and 6.30×10^{-25} cm^6/GW^2, respectively, in the femtosecond region, among the highest ones reported for many diphenylaminofluorene-based AFX chromophores and C_{60}-DPAF conjugates. Nonlinear absorption sensitivity was observed to increase by a factor of nearly 2.5 by extending molecular structural branching from the fullerenyl monoadduct to its bisadduct analogue containing two sterically hindered alkyl chains at the C_9 position of the fluorene ring.

Attachment of two hindered 3,5,5-trimethylhexyl groups in the structure of **3** improves its solubility and, concurrently, frustrates direct intermolecular stacking contact of fullerene cages and diphenylaminofluorene rings. Construction of C_{60}-(>DPAF-C_9)$_2$ triads was also coupled with the use of highly fluorescent DPAF-C_9 addends as primary antenna components to harvest light energy during either single-photon or two-photon excitation processes, leading to the formation of singlet excited-state C_{60}[>^{1}(DPAF-C_9)*]. Using nanosecond laser flash photolysis results taken at 355 nm as the reference for comparison, the transient absorption data obtained from femtosecond pump−probe experiments at 800 nm unambiguously substantiated the occurrence of two-photon excitation processes of C_{60}(>DPAF-C_9) in air-saturated benzene in the 100 fs-region. Subsequent efficient energy transfer from the two-photon pumped DPAF-C_9 moiety in C_{60}[>^{1}(DPAF-C_9)*] transient state to the C_{60} cage moiety occurred in the ns-region. These conclusions were made from the observation of T_1-T_n transient absorption of triplet excited state ^{3}(C_{60}>)* at 700−750 nm in a time scale of 1268 ps after short laser pulse excitation.

Photoinduced energy transfer from a donor moiety to the C_{60} cage in a C_{60}-donor conjugate structure could provide a plausible mechanism to drive the effective generation of singlet oxygen. Utility of C_{60} derivatives in single-photon excitation-based photodynamic tumor therapy (PDT) was demonstrated via in vivo studies.[23] Their efficacy was correlated to the ability of C_{60} hydrophilics in the generation of reactive singlet oxygen upon photoexcitation.[24] The use of a two-photon absorption (2PA) excitation process as an alternative PDT treatment procedure is advantageous because of its ability to focus on a confined small treatment area of diseased tissues in a greater depth and avoid causing damage to healthy surrounding tissues. The success of this approach relies heavily on the availability of stable multiphoton absorbing dyes with significantly large cross sections upon photoactivation. As the degree of conjugative molecular branching of substituted fluorene subunits becomes a crucial factor in enhancing 2PA and 3PA cross sections, the C_{60} cage may serve well as a nucleus center for building starburst fluorene dye components in designing MPA-active materials. The approach utilized in this study provided a reliable platform for probing the effect of starburst or dendritic chromophoric suprastructure on multiphoton absorptivity.

Acknowledgment. We thank Air Force Office of Scientific Research under the contract number FA9550-05-1-0154 and Materials & Manufacturing Directorate, Air Force Research Laboratory, for financial support of this work. We also thank Evgeny Danilov and Michael Rodgers for use of the femtosecond transient absorption instrumentation at the Ohio Laboratory for Kinetic Spectrometry located at Bowling Green State University.

Supporting Information Available: FAB$^+$ mass spectrum and ^{1}H NMR spectra of C_{60}(>DPAF-C_9) and C_{60}(>DPAF-C_9)$_2$ and ^{13}C NMR spectra of C_{60}(>DPAF-C_2) and C_{60}(>DPAF-C_9). This material is available free of charge via the Internet at http://pubs.acs.org.

CM060718Z

(23) (a) Yasuhiko, T.; Murakami, Y.; Ikada, Y. *Jpn. J. Cancer Res*. **1997**, *88*, 1108. (b) Yu, C.; Canteenwala, T.; Chen, H. H. C.; Chen, B. J.; Canteenwala, M.; Chiang, L. Y. *Proc. Electrochem. Soc*. **1999**, *12*, 234. (c) Yu, C.; Canteenwala, T.; Chen, H. C.; Jeng, U. S.; Lin, T. L.; Chiang, L. Y. In *Perspectives of Fullerene Nanotechnology*; Osawa, E., Ed.; Kluwer Academic Publisher: U.K., 2002; pp 165−183.

(24) Yu C.; Canteenwala, T.; El-Khouly, M. E.; Araki, Y.; Chiang, L. Y.; Wilson, B. C.; Ito, O.; Pritzker, K. *J. Mater. Chem*. **2005**, *15*, 1857−1864.